



Bernstein copula-based spatial cosimulation for petrophysical property prediction conditioned to elastic attributes

Van Huong Le^{a,*}, Martín A. Díaz-Viera^b, Daniel Vázquez-Ramírez^a, Raúl del Valle-García^b, Arturo Erdely^c, Dario Grana^d

^a Posgrado de Ciencias de la Tierra, Universidad Nacional Autónoma de México, Circuito de Posgrado S/N, Coyoacán, Ciudad Universitaria, 04510 Ciudad de México, Mexico

^b Instituto Mexicano del Petróleo, Eje Central Lázaro Cárdenas No. 152, Col. San Bartolo Atepehuacan, 07730 Ciudad de México, Mexico

^c Universidad Nacional Autónoma de México, FES Acatlán, Avenida Alcanfores y San Juan Totoltepe S/N, Sta Cruz Acatlan, 53150 Naucalpan de Juárez, Mexico

^d University of Wyoming, Department of Geology and Geophysics, Laramie, 82071 Wyoming, USA

ARTICLE INFO

Keywords:

Petrophysical properties
Elastic attributes
Joint distribution
Bernstein copula
Sequential Gaussian method
Stochastic simulation

ABSTRACT

A new methodology for the simulation of spatially distributed petrophysical properties conditioned by elastic attributes as secondary variables is presented. The method, namely Bernstein copula-based spatial cosimulation (BCSCS), is based on Bernstein copula for the estimation of the joint probability function and simulated annealing for the spatial simulation. The proposed method can model complex non-linear relationships between variables in a fully nonparametric approach. The main advantage is that it does not require linear dependence between variables nor any distribution constraint. This method is first validated in a 1-dimensional case at the well-log scale and it is applied in a 2-dimensional case at the seismic scale to predict effective porosity conditioned to P-impedance in a marine hydrocarbon reservoir located offshore Mexico. The uncertainty quantification analysis shows that the BCSCS method significantly reduces the uncertainty compared to the traditional sequential Gaussian cosimulation method.

1. Introduction

Petrophysical modeling in reservoir characterization consists of predicting petrophysical properties and their spatial configuration within the reservoir model (Cosentino, 2001). These properties cannot be measured directly in the reservoir, and they are usually inferred from other measurements (e.g. elastic attributes). Petrophysical property modeling in hydrocarbon reservoirs is challenging because of the limited amount of data available and the uncertainty in the measurements. For this reason, in recent years, stochastic simulation approaches have been adopted for the spatial distribution of petrophysical properties (Yarus and Chambers, 1994; Deutsch, 2002; Dubrule, 2003; Caers, 2005; Coburn et al., 2006; Doyen, 2007).

Seismic attributes are commonly used as secondary variables for predicting and statistical simulating rock and fluid properties. Among the estimation methods, the most common approaches are regression models (Chatterjee et al., 2016; Yenwongfai et al., 2017), neural networks (Iturrarán-Viveros, 2012; Iturrarán-Viveros and Parra, 2014; Alfarraj and AlRegib, 2018; Gogoi and Chatterjee, 2019; Maurya and Singh, 2019), and cokriging (Doyen et al., 1996; Babak and Deutsch,

2009; Moon et al., 2016; Xu et al., 2016). Spatial estimation methods have several disadvantages; since they require a large amount of data, produce smoothed results underestimating the variability due to natural heterogeneities, do not reproduce statistical properties, and do not give a systematic way to quantifying the uncertainty.

To overcome these challenges, spatial simulation methods have been proposed (Yarus and Chambers, 1994; Deutsch, 2002; Dubrule, 2003; Caers, 2005; Coburn et al., 2006; Doyen, 2007; Horta and Soares, 2010; Chilès and Delfiner, 2012). The most common simulation methods are sequential Gaussian cosimulation (SGCS) (Gómez-Hernández and Journel, 1993; Verly, 1993; Almeida and Journel, 1994; Parra and Emery, 2013; Emery and Parra, 2013; Verly, 1993; Almeida and Journel, 1994; Parra and Emery, 2013; Emery and Parra, 2013; Cao et al., 2014; Afshari and Shadizadeh, 2015), direct sequential cosimulation (Soares, 2001, 2005; Horta and Soares, 2010; Azevedo and Soares, 2017; Soares et al., 2017), simulated annealing cosimulation (Deutsch and Cockerham, 1994a,b; Vejbaek and Kristensen, 2000; Dafflon and Barrash, 2012), Gaussian mixture cosimulation

* Corresponding author.

E-mail addresses: levanhuong15011989@gmail.com (V.H. Le), mdiazv@imp.mx (M.A. Díaz-Viera), daniel_geofisico89@hotmail.com (D. Vázquez-Ramírez), rvalleg@imp.mx (R. del Valle-García), arturo.erdely@comunidad.unam.mx (A. Erdely), dgrana@uwo.edu (D. Grana).

<https://doi.org/10.1016/j.petrol.2020.107382>

Received 29 November 2019; Received in revised form 19 April 2020; Accepted 4 May 2020

Available online 8 May 2020

0920-4105/© 2020 Elsevier B.V. All rights reserved.

(Grana and Rossa, 2010; Grana et al., 2012, 2017; Lang and Grana, 2017; Figueiredo et al., 2019), and nonparametric mixture approach using kernel smoothing (Grana, 2018; Corina and Hovda, 2018). Spatial simulation methods reproduce the spatial variability and statistical properties; as they are often used for uncertainty quantification and do not depend on large dataset availability (Doyen, 2007).

The SGCS method assumes stationary random functions and it is generally applied with a linear co-regionalization model (Chilès and Delfiner, 2012). These assumptions imply a linear dependence between the primary and secondary variables. An extension of the SGCS method is the GauMix method where the model distribution is assumed to be a linear combination of multiple Gaussian pdfs. However, Gaussian distributions and the linear assumption do not correctly capture the dependency relationships between the variables in the real dataset.

For this reason, we present the Bernstein copula-based method that can correctly capture and reproduce complex relationships between variables without any assumptions of linearity or Gaussian distribution. Copulas have become popular in the financial sector to model complex data relationships and have been recently applied in geosciences (Díaz-Viera and Casar-González, 2005; Bárdossy, 2006; Bárdossy and Li, 2008; Stien and Kolbjørnsen, 2008; Kazianka and Pilz, 2010; Haslauer et al., 2010; Erdely and Díaz-Viera, 2010; Gräler and Pebesma, 2011; Hernández-Maldonado et al., 2012, 2014; Gräler, 2014; Erdely and Díaz-Viera, 2015; Bevacqua et al., 2017; Krupskii and Genton, 2019). There are two approaches to estimate the joint dependence based on parametric and nonparametric copula.

In the published literature, there are examples of parametric copula approach by several authors. Díaz-Viera and Casar-González (2005) and Díaz-Viera et al. (2006) applied copula using dependency measures such as Kendall and Spearman to simulate permeability using porosity as secondary variable; Bárdossy and Li (2008) applied a Gaussian copula for spatial interpolation of nitrate concentration; Kazianka and Pilz (2010) applied a Gaussian copula for spatial interpolation of benchmark geostatistical dataset; Erdely and Díaz-Viera (2015) applied a Vine trivariate parametric copula to predict permeability conditioned to porosity and P wave velocity. The nonparametric approach has been developed primarily by Erdely and Díaz-Viera (2010) and Hernández-Maldonado et al. (2012), who applied the bivariate Bernstein copula to predict permeability conditioned to porosity; Hernández-Maldonado et al. (2014) applied the trivariate Bernstein copula to predict permeability conditioned to porosity and S-wave velocity; Díaz-Viera et al. (2017) applied Bernstein copula to predict total porosity conditioned to P-impedance in 2D applications.

This work is a natural extension of the approach by Díaz-Viera et al. (2017) and shows the application of the BCSCS method to reservoir properties modeling conditioned to elastic attributes. The methodology is based on realizations obtained using the simulated annealing method where the joint probability distribution is estimated by a Bernstein nonparametric copula. The novelty of this work is in the use of the Bernstein copula method for geophysical inverse problems. It combines the inference of joint cumulative distribution function with the simulation annealing method to predict geostatistical realizations of reservoir properties. Furthermore, this approach is extended to multidimensional problems with applications to 2D sections of seismic attributes. The methodology is first described. Then, the method validation in a 1-dimensional case is presented using well log data and the advantages of BCSCS are shown through a comparison with SGCS. Finally, a case study in a 2-dimensional space along a seismic survey line are presented and discussed for the prediction of effective porosity conditioned to P-impedance at the seismic scale to a marine reservoir dataset acquired in the Gulf of Mexico.

2. Methodology

The proposed methodology aims to predict the petrophysical variables conditioned by elastic properties and generate geostatistical realizations that represent the spatial variability of the property. The

method includes two main parts: first the joint distribution of petrophysical and elastic variables is inferred from the available data using Bernstein copula, then these distributions are used to sample geostatistical realizations of the petrophysical properties conditioned by elastic measurements by combining the previously obtained distributions with simulated annealing. The workflow is summarized in Fig. 1.

The Bernstein copula-based spatial cosimulation (BCSCS) consists of capturing the univariate and bivariate probability distribution functions by approximating the Bernstein polynomial in its univariate empirical functions and empirical copula. Then, the global optimization method is applied through simulated annealing to reproduce the spatial dependence function.

Introduction to copulas

According to Sklar's theorem in Sklar (1959): Let H be a bivariate joint distribution function and F and G be the marginal distributions. A copula is a function $C: [0, 1]^2 \rightarrow [0, 1]$ such that for all x, y in \mathbf{R} ,

$$H(x, y) = C(F(x), G(y)) \quad (1)$$

If F and G are continuous, then C is unique; otherwise, C is uniquely determined on $RanF \times RanG$. Copula associated to a bivariate random vector (X, Y) describes the relationship between X and Y .

Let $F(x) = u, G(y) = v$. According to Nelsen (2006) and Joe (2014), the properties of copulas are:

1. $u = C(u, 1)$;
2. $v = C(1, v)$;
3. $C(0, v) = C(v, 0) = 0$;
4. For each u_1, u_2, v_1, v_2 in $\mathbb{I} = [0, 1]$ such that $u_1 \leq u_2$ and $v_1 \leq v_2$ then:
 $C(u_2, v_2) - C(u_1, v_2) - C(u_2, v_1) + C(u_1, v_1) \geq 0$;
5. The random variables u y v are independent if and only if $C(u, v) = \Pi(u, v) = uv$;
6. $W(u, v) \leq C(u, v) \leq M(u, v)$ where $W(u, v) = \max(u + v - 1, 0)$ and $M(u, v) = \min(u, v)$ are also copulas.
7. $0 \leq \frac{\partial}{\partial u} C(u, v) \leq 1$ and $0 \leq \frac{\partial}{\partial v} C(u, v) \leq 1$;
8. $u \mapsto \frac{\partial C(u, v)}{\partial v}$ and $v \mapsto \frac{\partial C(u, v)}{\partial u}$ are nondecreasing;
9. The copula density function: $c(u, v) = \frac{\partial^2 C(u, v)}{\partial u \partial v}$ exists when C is absolutely continuous.

Let $S = \{(x_1, y_1), (x_2, y_2), \dots, (x_n, y_n)\}$ be observations of the random variables X and Y , where X is the elastic attribute and Y is the petrophysical property. Georeferenced random variables are characterized by joint and univariate cumulative distribution functions $H(x, y)$, $F(x)$, $G(y)$, and the spatial correlation function (γ). Once these functions are known then the variables can be simulated.

From the observations of S , the empirical univariate cumulative distribution functions $F_n(x)$ and $G_n(y)$ of X and Y , respectively, are estimated by:

$$F_n(x) = \frac{1}{n} \sum_{k=1}^n \mathbb{I}\{x_{(k)} \leq x\}, \quad G_n(y) = \frac{1}{n} \sum_{k=1}^n \mathbb{I}\{y_{(k)} \leq y\} \quad (2)$$

where \mathbb{I} represents an indicator function equal to 1 when its argument is true, and 0 otherwise.

The empirical copula is a function C_n with domain $\{\frac{i}{n}; i = 0, 1, \dots, n\}^2$ defined as:

$$C_n\left(\frac{i}{n}, \frac{j}{n}\right) = \frac{1}{n} \sum_{k=1}^n \mathbb{I}\{\text{rank}(x_k) \leq i, \text{rank}(y_k) \leq j\} \quad (3)$$

The functions F_n , G_n and C_n are step functions while X and Y are continuous variables. Hence, a smoothing technique is necessary. Several smoothing methods are available, such as B-spline (Shen et al., 2008), Kernel density (Nagler and Czado, 2016), Bernstein polynomial (Erdely and Díaz-Viera, 2010), etc. In this method, we use Bernstein polynomial because of its analytical tractability.

The univariate quantile function $Q(u)$ of the random variable X :

$$Q(u) = F^{-1}(u) = \inf\{x : F(x) \geq u\}, \quad 0 \leq u \leq 1 \quad (4)$$

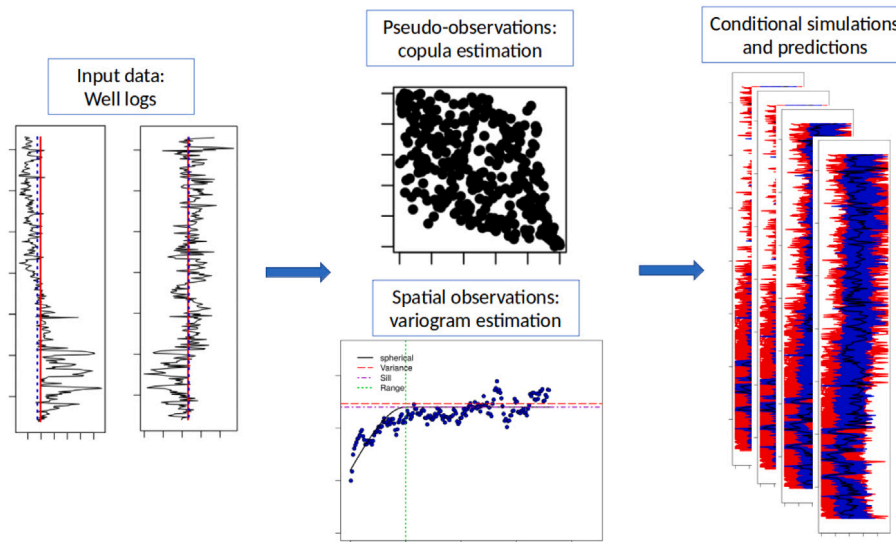


Fig. 1. Workflow of the methodology.

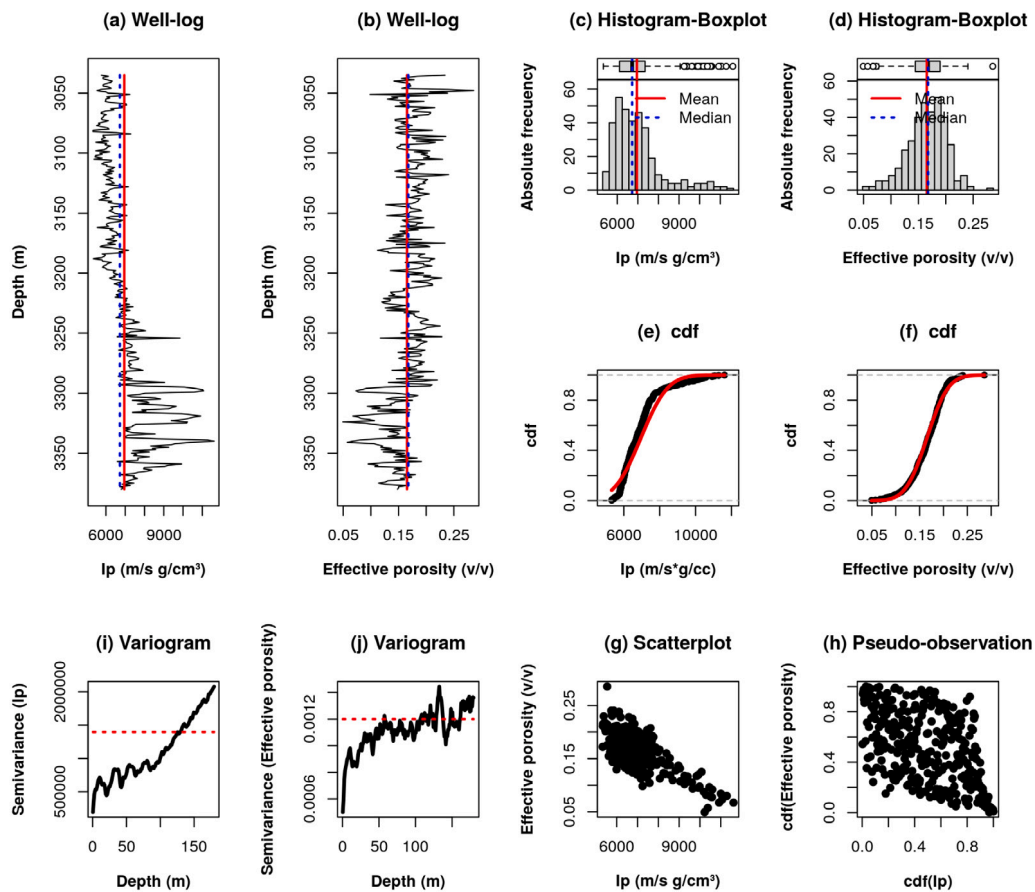


Fig. 2. (a) and (b): Well-log, (c) and (d): Histogram-boxplot, (e) and (f): Empirical (in black) and normal (in red) cumulative distribution function (cdf), (g) and (h): Scatterplot and Pseudo-observation, (i) and (j): Experimental semivariogram (in black) and variance (in dashed red) of P-Impedance and effective porosity. (For interpretation of the references to color in this figure legend, the reader is referred to the web version of this article.)

can be approximated using Bernstein polynomials as (Perez and Palacín, 1987):

$$\tilde{Q}(u) = \sum_{k=0}^n \frac{1}{2} (x_{(k)} + x_{(k+1)}) \binom{n}{k} u^k (1-u)^{n-k} \quad (5)$$

Similarly the univariate quantile function of the random variable Y can be derived.

Moreover, a smooth extension can be derived using Bernstein copula:

$$\tilde{C}(u, v) = \sum_{i=0}^n \sum_{j=0}^n C_n \left(\frac{i}{n}, \frac{j}{n} \right) \binom{n}{i} u^i (1-u)^{n-i} \binom{n}{j} v^j (1-v)^{n-j} \quad (6)$$

for each (u, v) in the unit square $[0, 1]^2$, and where C_n is as defined in Eq. (3) (Sancetta and Satchell, 2004) y (Sancetta, 2007).

From Eq. (1) to Eq. (6), the univariate and bivariate cumulative distribution functions $H(x, y)$, $F(x)$, $G(y)$ are estimated. These distributions are inferred from the data and are then used to generate geostatistical realizations of the reservoir properties, conditioned by the geophysical measurements.

Conditional simulation algorithm

To simulate realizations from the random variables X and Y according to the measured data $S = \{(x_1, y_1), \dots, (x_n, y_n)\}$, we follow the algorithm in Nelsen (2006):

1. Generate continuous random variables u and t uniformly distributed in $[0, 1]$.
2. Set $v = c_u^{-1}(t)$ where

$$c_u(v) = \frac{\partial \tilde{C}(u, v)}{\partial u} \quad (7)$$

and \tilde{C} is computed as in Eq. (6).

3. The couple is $(x, y) = (\tilde{Q}_n(u), \tilde{R}_n(v))$, where \tilde{Q}_n y \tilde{R}_n are the smoothed quantile functions of X, Y , in Eq. (5).
For a value x of the random variable X and $0 < \alpha < 1$ let $y = \varphi_\alpha(x)$ be the solution of

$$P(Y \leq y | X = x) = \alpha. \quad (8)$$

Then the graph of $y = \varphi_\alpha(x)$ is the α -quantile regression curve of Y conditioned to $X = x$. Nelsen (2006), shows that

$$P(Y \leq y | X = x) = c_u(v)|_{u=F(x), v=G(y)}, \quad (9)$$

The results of Eqs. (7)–(9) leads to the algorithm for the α -quantile regression curve of Y conditioned to $X = x$:

1. Set $c_u(v) = \alpha$.
2. Solve for $v = g_\alpha(u)$.
3. Substitute u by $\tilde{Q}_n^{-1}(x)$ and v by $\tilde{R}_n^{-1}(y)$.
4. Solve for $y = \varphi_\alpha(x)$.

Further details can be found in Erdely and Díaz-Viera (2010), Hernández-Maldonado et al. (2012, 2014), Mendoza-Torres et al. (2017) and Díaz-Viera et al. (2017).

The algorithms allows modeling the univariate and bivariate probability distribution functions of the properties of interest. However, the simulation of the properties in the spatial domain requires a spatial correlation function (i.e. the semivariogram). Simulated annealing is then used for the stochastic spatial simulation of the properties of interest, using a semivariogram model as objective function (Deutsch and Cockerham, 1994a,b; Deutsch and Journel, 1998). At this stage, optimization is required so that the spatial distribution function (semivariogram) of the petrophysical property of interest (Y) converges to the proposed semivariogram. The procedure consists in reducing the difference between the simulated semivariogram $\gamma^*(h)$ and the reference semivariogram $\gamma(h)$ in Eq. (10), by minimizing the following objective function

$$FO = \sum_h \left[\frac{\gamma^*(h) - \gamma(h)}{\gamma(h)} \right]^2 \quad (10)$$

Table 1
Descriptive statistics of the measured data.

Statistics	P-impedance	Effective porosity
Minimum	5324.4324	0.0493
Median	6723.4581	0.1677
Mean	6953.9369	0.1654
Maximum	11,612.4245	0.2857
Variance	139,5507.9379	0.0012
Skewness	1.5870	-0.4323

Uncertainty quantification

Given a value of the seismic attribute $X = x$, a range of possible values of the petrophysical property $Y = y \pm \Delta y$ at the spatial point of interest will be predicted. 100 simulations of the primary variable Y are obtained and then validated with the reference values of Y . The simulations Y^* are conditioned to the secondary variable X applying two cosimulation methods: traditional SGCS and proposed BCSCS. The uncertainty ranges were compared to the reference Y values. In addition, the descriptive statistics, the probability distribution functions and the spatial distribution functions of the sets of 100 simulations Y^* were compared to the reference solution.

The general workflow included (1) exploratory data analysis, (2) variographic analysis, (3) simulations, and (4) uncertainty quantification.

3. Validation case

The BCSCS method is validated and compared with the SGCS method in a 1-dimensional case using well-log data from an offshore field, in the province of the Mexican Cordilleras, Mexico. The main reservoir includes a sequence of shale and sand. The petrophysical property, effective porosity, and the elastic attribute, P-impedance (Ip), come from the logs of a well with a sampling interval of 1 m and a depth from 3035 m to 3380 m. P-impedance is used as conditioning variable to simulate effective porosity. The simulated effective porosity is validated with the reference data at the well-log scale.

First, we infer the joint distributions from the available data, then we simulate the petrophysical properties conditioned by the elastic properties and compare with the results with the data at the well location.

3.1. Exploratory data analysis

Fig. 2(a) and (b) show the spatial distribution, mean, and median of the reference data. P-impedance shows a moderate depth trend. We assume that porosity is stationary since the local mean and variance do not vary with the coordinates (Díaz-Viera, 2002).

Table 1 shows the statistics of P-impedance and effective porosity. Fig. 2(c), (d), (e), and (f) show that the univariate probability distribution of P-impedance is skewed whereas effective porosity is close to be unimodal and symmetric. Fig. 2(c), (d), (e), and (f) show the existence of outliers.

In Table 2, Fig. 2(g), and (h), it is observed that P-impedance and effective porosity show an average negative correlation, which means that, in general, as the P-impedance increases, effective porosity decreases. Fig. 2(g) shows the scatterplot of the variables. Fig. 2(h) shows the pseudo-observation in the range of empirical cumulative distribution functions (cdf), from 0 to 1. In addition, the pseudo-observation is a representation of the copula. According to Sklar (1959), the copula contains the information of joint dependence between the variables, and the copula is independent of the marginal functions.

Table 2 shows that the Spearman and Kendall correlation coefficients are consistent in the data and pseudo-observation domains, whereas the Pearson's correlation coefficient changes.

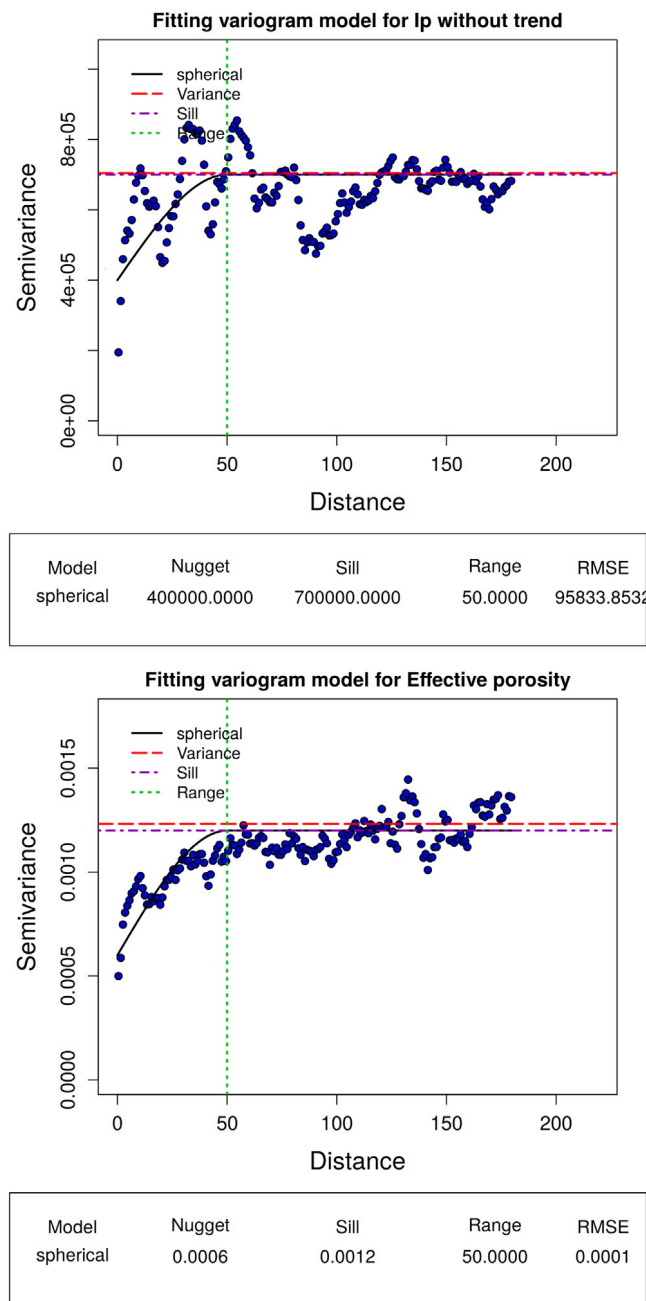


Fig. 3. Semivariogram models and empirical semivariogram for P-impedance and effective porosity in depth direction.

Table 2
Correlation coefficients.

Coefficients	Observation domain	Pseudo-observation domain
Pearson	-0.7078	-0.5603
Spearman	-0.5603	-0.5603
Kendall	-0.4051	-0.4051

3.2. Variographic analysis

When the semivariogram is bounded to the extent of the variance, then it is said that the variable has at least second-order stationarity (Díaz-Viera, 2002).

Fig. 2(i) and (j) show that P-impedance has non-stationary behavior, because its semivariogram grows with the square of the depth. In order

Table 3

Statistics of 100 simulations of effective porosity by SGCS and BCSCS, and reference effective porosity.

Statistics	BCSCS	Reference data	SGCS
Minimum	0.0493	0.0493	0.0492
Median	0.1688	0.1677	0.1673
Mean	0.1654	0.1654	0.1631
Maximum	0.2856	0.2857	0.2858
Variance	0.0012	0.0012	0.0020
Skewness	-0.4691	-0.4323	-0.3331

to estimate a semivariogram model for P-impedance, it is necessary to remove the trend. In Fig. 3, the estimated semivariogram model for P-impedance and effective porosity is presented. The correlation range is approximately 50 m. This assumption complies with the assumption of the linear co-regionalization model of the traditional SGCS method (Chilès and Delfiner, 2012).

The semivariogram model of the effective porosity $\gamma(h)$ is a spherical model with a nugget equal to 0.0006, a sill equal to 0.0012, and a scope equal to 50.0 m.

3.3. Bernstein copula-based spatial cosimulation

Fig. 4 shows that empirical cdf of P-impedance and effective porosity are step functions (in black), but P-impedance and the effective porosity are continuous variables. Therefore, a smoothing technique is necessary for those functions. According to the methodology, the empirical cdf of P-impedance and effective porosity are approximated by Bernstein polynomial through Eq. (5). Fig. 4 shows the results of the approximation and also illustrates that Bernstein polynomial fits well to the empirical cdf of P-impedance and effective porosity. For comparison, the parametric Gaussian cdf does not fit the P-impedance distribution (Fig. 4).

Fig. 5 shows the step function representing the empirical copula of P-impedance and effective porosity (in black). The empirical copula of P-impedance and effective porosity is approximated by Bernstein copula through Eq. (6) and is shown in Fig. 5.

Based on the previous results, 100 simulations of the effective porosity conditioned to P-impedance are simulated using the conditional simulation algorithm proposed in the methodology section.

To reproduce the semivariogram model, we apply the simulated annealing method with the objective functions in Eq. (10).

The proposed method is compared to sequential Gaussian cosimulation (SGCS) based on a conditioning Markov model available in the open source code SGeMS (Remy et al., 2009). The variable of interest is effective porosity and secondary variable is P-impedance without trend. 100 simulations of the effective porosity conditioned to P-impedance are simulated by SGCS using the same semivariogram model.

3.4. Uncertainty quantification

The simulations of the effective porosity conditioned to P-impedance obtained with the two simulation methods are compared and validated with the reference effective porosity. The univariate, bivariate, spatial distribution, as well as the modeling error the reference and simulated effective porosity are compared.

In Fig. 6(a), the empirical univariate cdf results of the BCSCS method (in blue) show the smaller uncertainty compared to those of the SGCS method (in red). Table 3 shows the statistics of results of 100 simulations of effective porosity by the two methods and the reference effective porosity. In particular, the variance of the results of the SGCS method is almost the double the variance of the results of the BCSCS method and the reference effective porosity.

Comparing the bivariate aspect through scatterplot and pseudo-observation, Fig. 6(b) and (c) show that the results of the BCSCS method (in blue) reproduce the property dependence better than the

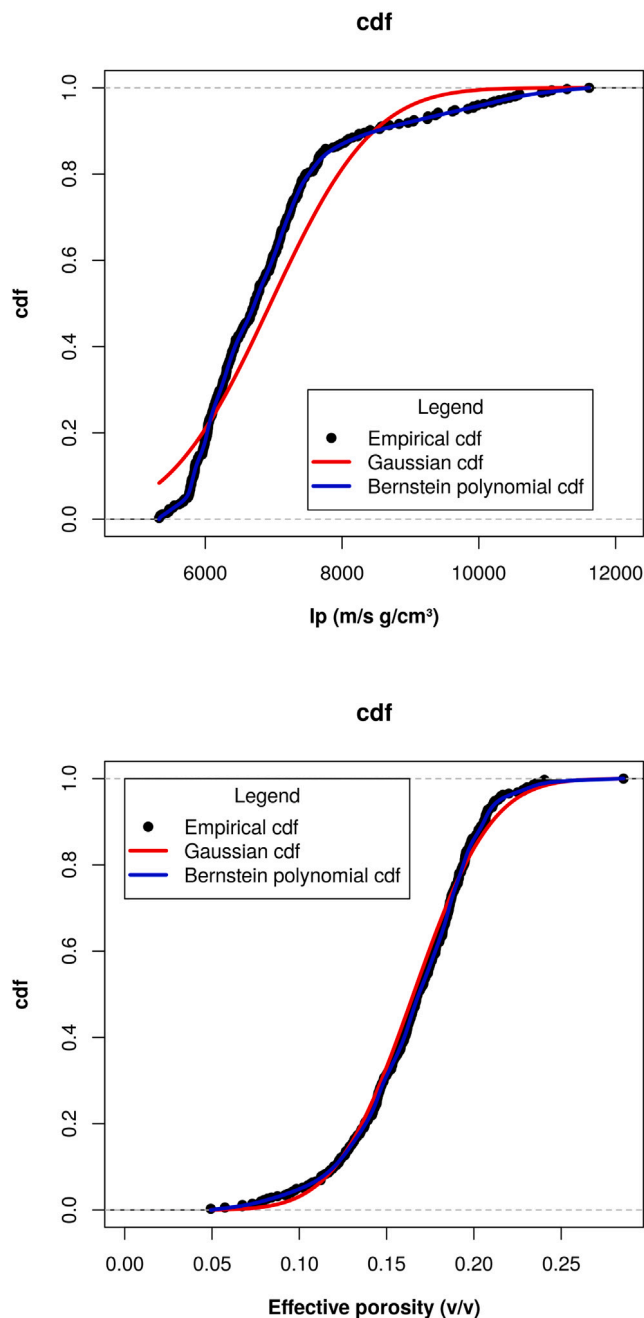


Fig. 4. Empirical cdf of P-impedance and effective porosity approximated using Bernstein polynomial (in blue) compared to Gaussian cdf with mean and standard deviation of the variable (in red). (For interpretation of the references to color in this figure legend, the reader is referred to the web version of this article.)

results of the SGCS method (in red), compared to the reference data (in black). Table 4 shows that the dependency coefficients (Pearson, Kendall, Spearman) of the BCSCS method are closer to the references than for the SGCS method. Therefore, the results of the bivariate behavior of the SGCS method show greater uncertainty compared to those of the BCSCS method.

In terms of the semivariogram model reproduction, Fig. 6(d) and (e) show that the uncertainty of 100 simulated effective porosity by the BCSCS method (in blue) is smaller than the results of the SGCS method (in red) with respect to the reference semivariogram and well-log data (in black). Moreover, Fig. 6(f) shows that the expected value of 100 simulations of effective porosity by BCSCS method matches the

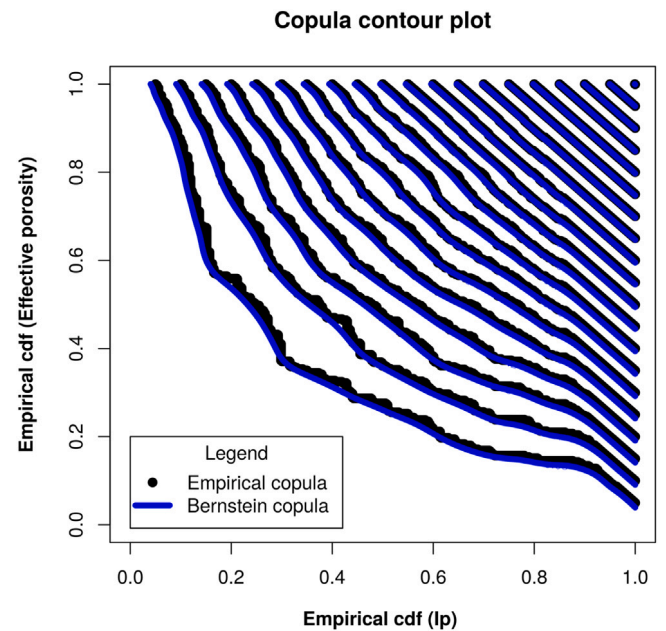


Fig. 5. Empirical copula and copula approximated by Bernstein copula of P-impedance and effective porosity.

Table 4

Correlation coefficients of P-impedance and effective porosity for BCSCS, reference data and SGCS.

Coefficients	BCSCS	Reference data	SGCS
Pearson	-0.6966	-0.7078	-0.5720
Spearman	-0.5491	-0.5603	-0.6275
Kendall	-0.3937	-0.4051	-0.4409

reference data. Therefore, the accuracy in Fig. 6(f) and precision in Fig. 6(e) improve with the BCSCS method.

Finally, the error between simulated values and reference data is analyzed. Table 5 and Fig. 7 show the histogram-boxplot and the statistics of the errors between the reference data and 100 simulations of effective porosity and confirm that the BCSCS method provides better results.

4. Application case

The proposed method is finally applied to an in-line section of inverted P-impedance section (Fig. 8(a)). The section shows a depth interval including sand and shale lithologies. P-impedance has been obtained from seismic inversion of amplitudes and travel-times, using a traditional convolutional method where the seismic response is assumed to be approximated as a convolution of the source wavelet and the reflection coefficients computed from P-wave velocity and density. The results of seismic inversion have been converted from time to depth by using the predicted seismic velocity. The low P-impedance in the upper part of the interval suggests a potential high-porosity reservoir. The goal of the application is to predict the effective porosity distribution along the 2D section. The well log data in the previous section are used to model the rock physics relation between P-impedance and effective porosity. Seismic data and seismic properties estimated from the data have a lower resolution than well log data due to the limited bandwidth of the acquisition frequencies. Therefore, the models obtained from

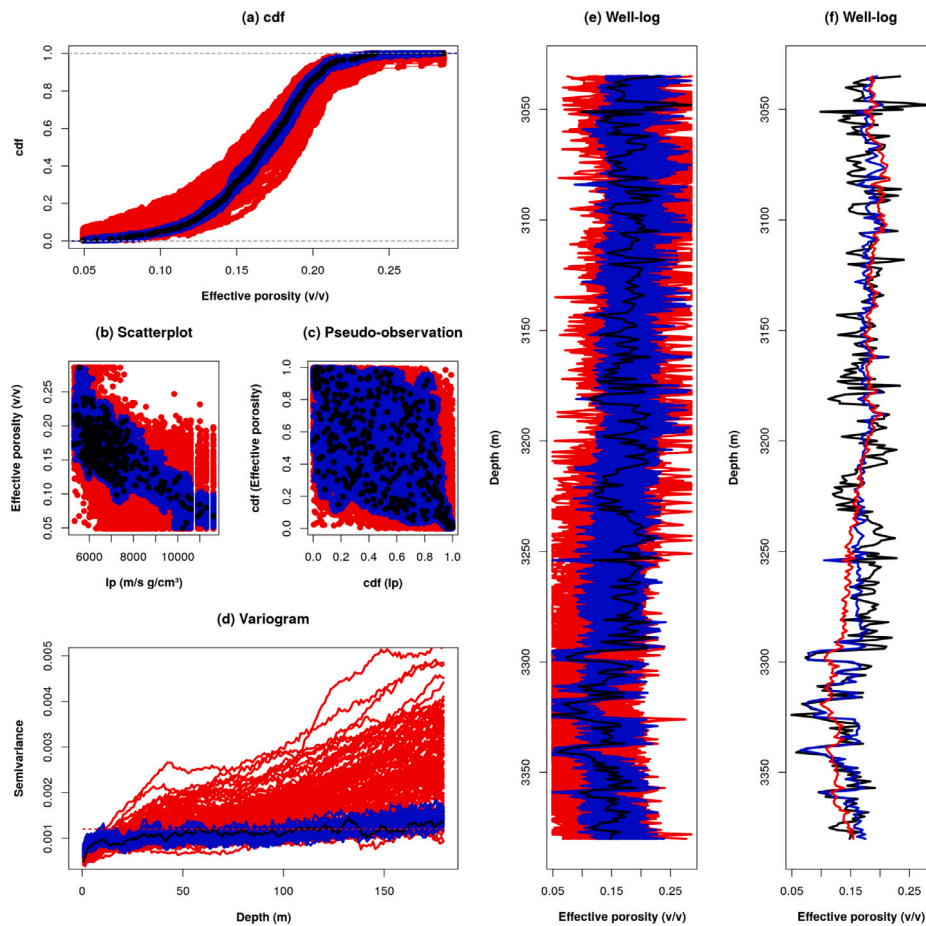


Fig. 6. (a) Empirical cdf of effective porosity, (b) Scatterplot of P-impedance versus effective porosity; (c) Pseudo-observation of cdf(P-impedance) versus cdf(effective porosity), (d) Variogram and (e) Well-log of effective porosity (reference in black, 100 simulations by BCSCS in blue, 100 simulations by SGCS in red and variance in dashed red), and (f) Well-log of effective porosity (reference in black, mean of 100 simulations by BCSCS in blue, mean of 100 simulations by SGCS in red). (For interpretation of the references to color in this figure legend, the reader is referred to the web version of this article.)

Table 5
Error statistics of BCSCS and SGCS.

Statistics	BCSCS	SGCS
Minimum	-0.1351	-0.2183
Median	0.0002	-0.0005
Mean	0.0001	-0.0023
Maximum	0.1305	0.1771
Variance	0.0012	0.0021
Absolute Sum	908.1104	1267.168

seismic data are typically smoother, in the vertical direction, compared to the corresponding well log data. The lateral continuity in the data is generally due to the geological continuity of the geobodies in the subsurface. The semivariograms are estimated from the P-impedance models. Fig. 9 shows the anisotropic behavior of the semivariograms of P-impedance in the vertical and lateral directions.

The BCSCS method is applied to predict effective porosity conditioned to inverted P-impedance at the seismic scale using their joint dependency model estimated at the well-log scale. This ensures that univariate and bivariate distributions of the effective porosity in the

well-log scale will be reproduced. The vertical and lateral semivariogram models of effective porosity are assumed to be similar to the directional semivariogram models of P-impedance, due to the correlation between the two properties shown in the well logs.

Fig. 8(b) and (c) show the median value and the standard deviation of 100 simulations of effective porosity conditioned to inverted P-impedance. The predicted model shows a high-porosity region in the upper part of the interval, that corresponds to the potential reservoir layer according to geological interpretation and nearby wells. The spatial structure of effective porosity is not identically the same as the spatial structure of P-impedance because the joint dependence between them is not linear. The semivariograms of the median value of 100 simulations of effective porosity in the vertical and lateral directions are shown in Fig. 10.

5. Conclusions

The proposed method, namely Bernstein copula-based spatial cosimulation, produces more accurate results compared to sequential Gaussian cosimulation method. Indeed, the BCSCS method can model the dependence between the random variables of interest, without assuming a linear dependence between variables nor parametric probability distribution functions.

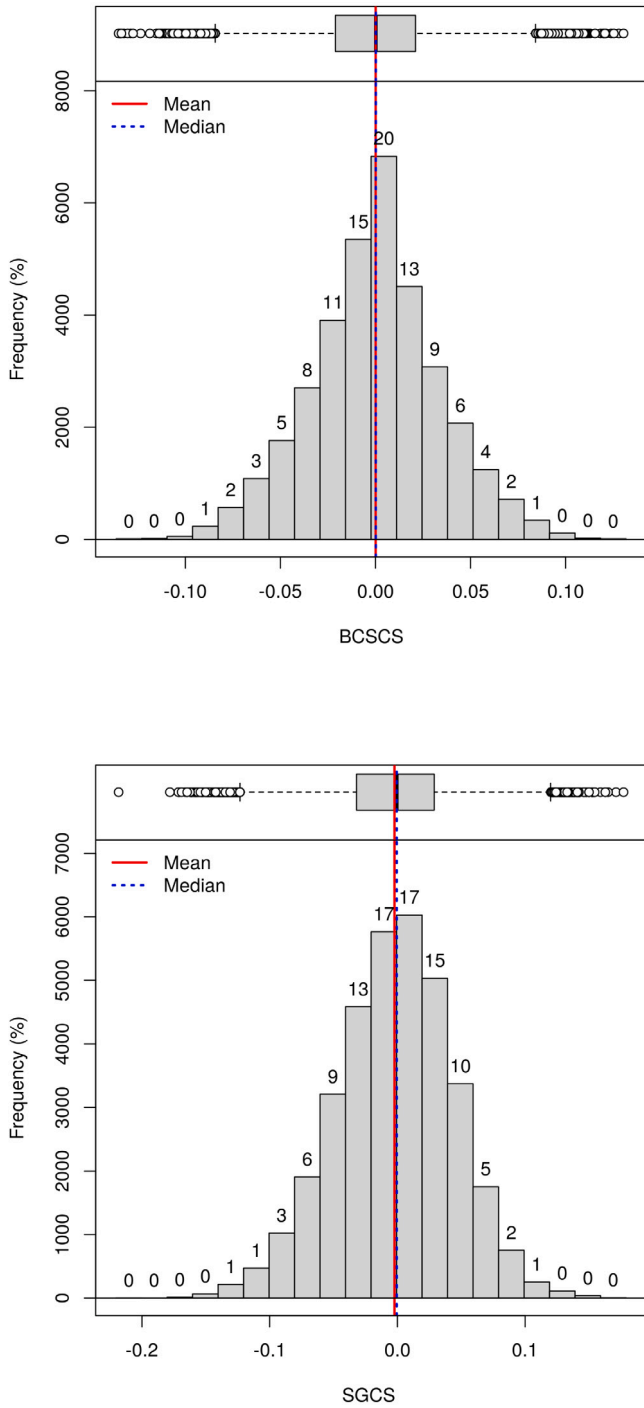


Fig. 7. Histogram-boxplot of errors of 100 simulations of effective porosity by BCSCS and SGCS.

The validation study shows that the BCSCS method provides more accurate results and more precise uncertainty quantification than standard simulation methods such as SGCS. The application showed an example of how the BCSCS method can be applied by combining the data from different scales, such as borehole and surface geophysics scale.

The proposed approach can be extended to multivariate problems with several elastic attributes to predict a set of reservoir proper-

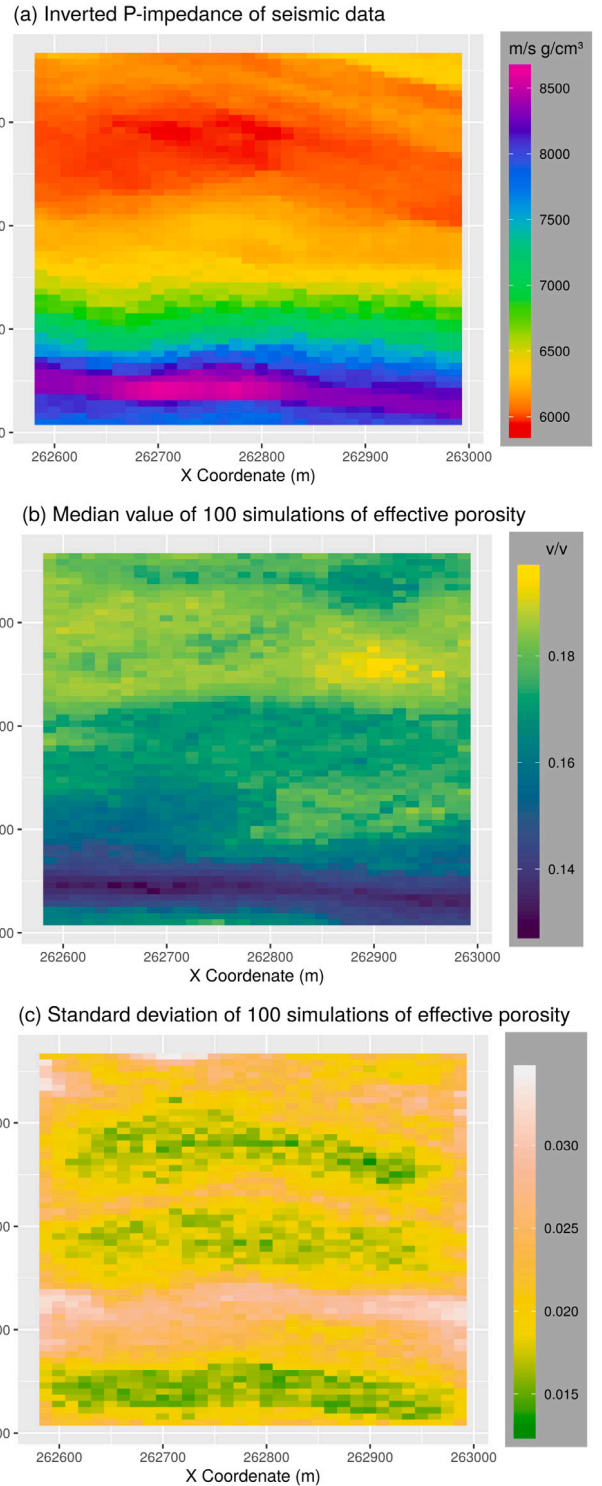


Fig. 8. (a) In-line section of inverted P-impedance of seismic data; (b) Median value and (c) Standard deviation of 100 simulations of effective porosity.

ties of interest, including porosity, mineralogy, and fluid saturations. This extension can be achieved by using multivariate copula or by applying standard multivariate statistical procedures or machine learning algorithms. Furthermore, the method can be implemented for 3-dimensional applications.

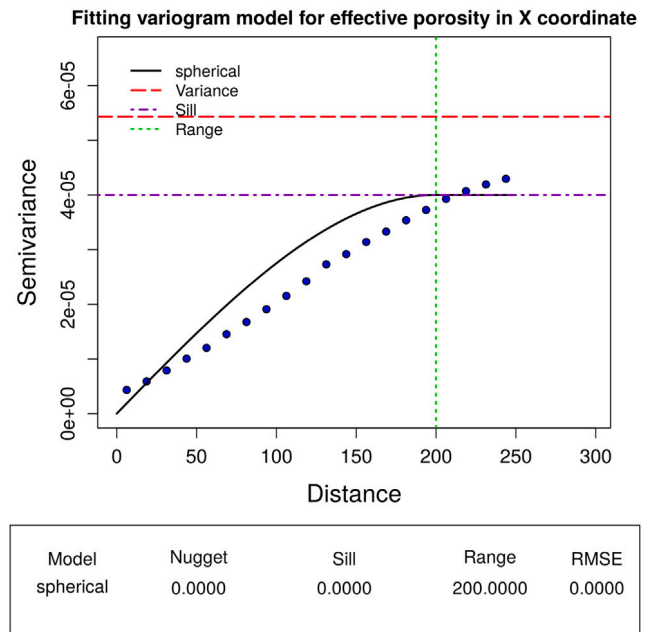
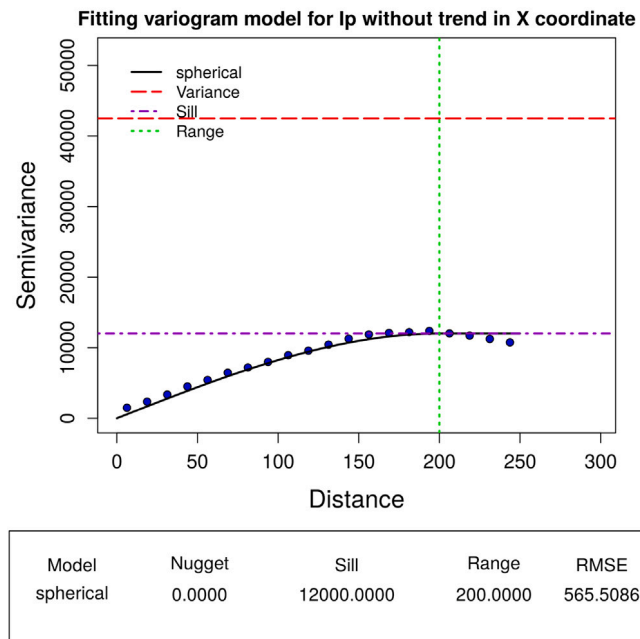
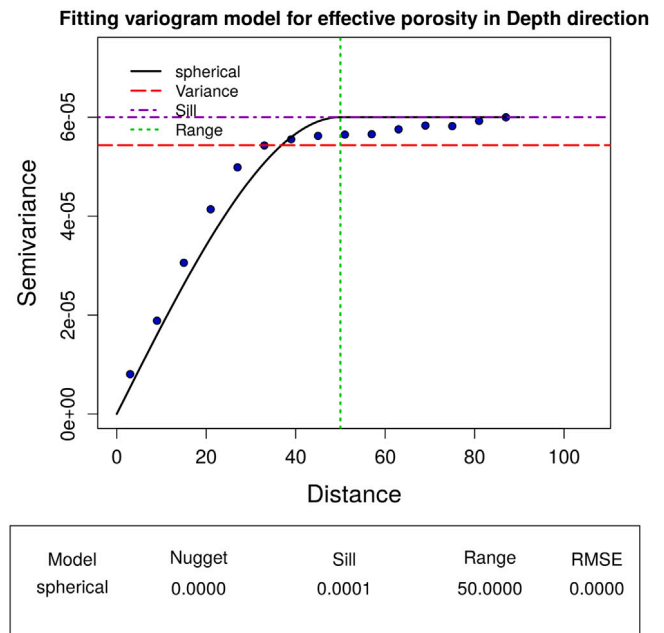
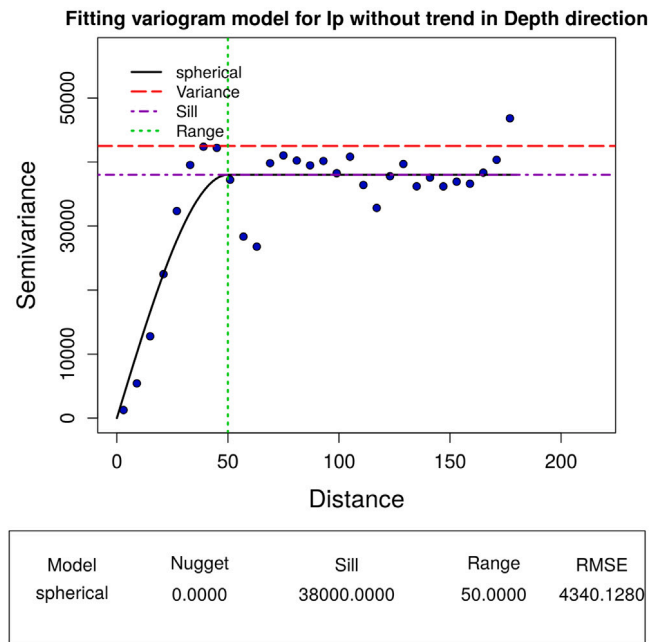


Fig. 9. Semivariogram models and empirical semivariogram of P-impedance along the in-line section.

Fig. 10. Semivariogram models and empirical semivariogram of the median value of 100 simulations of effective porosity.

CRedit authorship contribution statement

Van Huong Le: Validation, Formal analysis, Data curation, Writing - original draft, Visualization, Funding acquisition. **Martín A. Díaz-Viera:** Conceptualization, Methodology, Investigation, Supervision, Project administration, Writing - review & editing. **Daniel Vázquez-Ramírez:** Validation, Writing - review & editing. **Raúl del Valle-García:** Resources, Writing - review & editing. **Arturo Erdely:** Software, Writing - review & editing. **Dario Grana:** Project administration, Writing - review & editing.

Declaration of competing interest

The authors declare that they have no known competing financial interests or personal relationships that could have appeared to influence the work reported in this paper.

Acknowledgments

Ph.D. student Van Huong Le acknowledges CONACYT for the scholarship 705888 and Universidad Nacional Autónoma de México for supporting this research. The data were provided by the National Hydrocarbons Commission of Mexico, according to appendix C of the license to use the information in favor of Universidad Nacional Autónoma de México, dated December 11, 2017, under the nomenclature CNIH-C-00417. This reference information is the property of Mexico and

its collection, safekeeping, use, administration and updating, as well as its publication is only authorized to the National Hydrocarbons Commission.

References

- Afshari, A., Shadizadeh, S.R., 2015. Integration of petrophysical and seismic data to construct areal permeability model. *Energy Sources A* 679–686. <http://dx.doi.org/10.1080/15567036.2011.590863>.
- Alfarraj, M., AlRegib, G., 2018. Petrophysical property estimation from seismic data using recurrent neural networks. In: SEG Technical Program Expanded Abstracts 2018. Society of Exploration Geophysicists, pp. 2141–2146. <http://dx.doi.org/10.1190/segam2018-2995752.1>, URL <https://library.seg.org/doi/10.1190/segam2018-2995752.1>.
- Almeida, A.S., Journel, A.G., 1994. Joint simulation of multiple variables with a Markov-type coregionalization model. *Math. Geol.* 26 (5), 565–588. <http://dx.doi.org/10.1007/BF02089242>.
- Azevedo, L., Soares, A., 2017. Geostatistical Methods for Reservoir Geophysics. Springer International Publishing, <http://dx.doi.org/10.1007/978-3-319-53201-1>, URL <https://www.springer.com/gp/book/9783319532004>.
- Babak, O., Deutsch, C.V., 2009. Improved spatial modeling by merging multiple secondary data for intrinsic collocated cokriging. *J. Pet. Sci. Eng.* 69 (1), 93–99. <http://dx.doi.org/10.1016/j.petrol.2009.08.001>, URL <http://www.sciencedirect.com/science/article/pii/S0920410509001697>.
- Bárdossy, A., 2006. Copula-based geostatistical models for groundwater quality parameters. *Water Resour. Res.* URL <https://doi.org/10.1029/2005WR004754>.
- Bárdossy, A., Li, J., 2008. Geostatistical interpolation using copulas. <http://dx.doi.org/10.1029/2007WR006115>, URL <https://agupubs.onlinelibrary.wiley.com/doi/pdf/10.1029/2007WR006115>.
- Bevacqua, E., Maraun, D., Haff, I.H., Widmann, M., Vrac, M., 2017. Multivariate statistical modelling of compound events via pair-copula constructions: analysis of floods in Ravenna (Italy). *Hydrol. Earth Syst. Sci.* 21, 2701–2723. <http://dx.doi.org/10.5194/hess-21-2701-2017>.
- Caers, J., 2005. *Petroleum Geostatistics*. Society of Petroleum Engineers, URL <https://store.spe.org/Petroleum-Geostatistics-P45.aspx>.
- Cao, R., Ma, Y.Z., Gomez, E., 2014. Geostatistical applications in petroleum reservoir modelling. *J. South. Afr. Inst. Min. Metall.* URL http://www.scielo.org.za/scielo.php?script=sci_arttext&pid=S2225-62532014000800013.
- Chatterjee, R., Singha, D.K., Ojha, M., Sen, M.K., Sain, K., 2016. Porosity estimation from pre-stack seismic data in gas-hydrate bearing sediments, Krishna-Godavari basin, India. *J. Nat. Gas Sci. Eng.* 33, 562–572. <http://dx.doi.org/10.1016/j.jngse.2016.05.066>, URL <https://www.sciencedirect.com/science/article/pii/S1875510016303808>.
- Chilès, J.-P., Delfiner, P., 2012. *Geostatistics: Modeling Spatial Uncertainty*, second ed. John Wiley & Sons, Inc., Hoboken, New Jersey, <http://dx.doi.org/10.1002/9781118136188>.
- Coburn, T.C., Yarus, J.M., Chambers, R.L., 2006. *Stochastic Modeling and Geostatistics: Principles, Methods, and Case Studies*, Volume II, Vol. 5. American Association of Petroleum Geologists, <http://dx.doi.org/10.1306/CA51063>.
- Corina, A., Hovda, S., 2018. Automatic lithology prediction from well logging using kernel density estimation. *J. Pet. Sci. Eng.* 170, 664–674. <http://dx.doi.org/10.1016/j.petrol.2018.06.012>, URL <http://www.sciencedirect.com/science/article/pii/S0920410518304960>.
- Cosentino, L., 2001. *Integrated Reservoir Studies*. TECHNIP, Paris, France, URL <http://www.editionstechnip.com/en/catalogue-detail/695/integrated-reservoir-studies.html>.
- Dafflon, B., Barrash, W., 2012. Three-dimensional stochastic estimation of porosity distribution: benefits of using ground-penetrating radar velocity tomograms in simulated-annealing-based or Bayesian sequential simulation approaches. *Water Resour. Res.* <http://dx.doi.org/10.1029/2011WR010916>.
- Deutsch, C.V., 2002. *Geostatistical Reservoir Modeling*, first ed. Oxford University Press.
- Deutsch, C.V., Cockerham, P.W., 1994a. Geostatistical modeling of permeability with annealing cosimulation (ACS). In: SPE Annual Technical Conference and Exhibition, New Orleans, Louisiana, pp. 523–532. <http://dx.doi.org/10.2118/28413-MS>. URL <https://www.onepetro.org/conference-paper/SPE-28413-MS>.
- Deutsch, C.V., Cockerham, P.W., 1994b. Practical considerations in the application of simulated annealing to stochastic simulation. *Math. Geol.* 26 (1), 67–82. <http://dx.doi.org/10.1007/BF02065876>.
- Deutsch, C.V., Journel, A.G., 1998. *GSLIB: Geostatistical Software Library and User's Guide*, second ed. Oxford University Press, New York.
- Díaz-Viera, M.A., 2002. *Geostatística aplicada*. Instituto de Geofísica, UNAM. Instituto de Geofísica y Astronomía, CITMA, Cuba, URL <http://www.esmg-mx.org/media/courses/geoestadística/GeoEstadística.pdf>.
- Díaz-Viera, M.A., Anguiano-Rojas, P., Mousatov, A., Kazatchenko, E., Markov, M., 2006. Stochastic modeling of permeability in double porosity carbonates applying a Monte-Carlo simulation method with t-copula. In: SPWLA 47th Annual Logging Symposium. URL <https://www.onepetro.org/download/conference-paper/SPWLA-2006-00?id=conference-paper%2FSPWLA-2006-00>.
- Díaz-Viera, M.A., Casar-González, R., 2005. Stochastic simulation of complex dependency pattern of petrophysical properties using T-copulas. In: Proceedings of IAMG'05: GIS and Spatial Analysis, Vol. 2. pp. 749–755, URL https://link.springer.com/chapter/10.1007/978-3-642-12465-5_13.
- Díaz-Viera, M.A., Erdely, A., Kerdan, T., del Valle-García, R., Mendoza-Torres, F., 2017. Bernstein copula-based spatial stochastic simulation of petrophysical properties using seismic attributes as secondary variable. In: Gómez-Hernández, J., Rodrigo-Ilari, J., Rodrigo-Clavero, M., Cassiraga, E., Vargas-Guzmán, J. (Eds.), *Geostatistics Valencia 2016*. In: Quantitative Geology and Geostatistics, vol. 19, Springer, Cham, pp. 487–504. http://dx.doi.org/10.1007/978-3-319-46819-8_33.
- Doyen, P., 2007. *Seismic Reservoir Characterization: An Earth Modelling Perspective*. European Association of Geoscientists and Engineers, URL <https://bookshop.eage.org/product/seismic-reservoir-characterization-an-earth-modelling-perspective-eet-2/>.
- Doyen, P.M., den Boer, L.D., Pillet, W.R., 1996. Seismic porosity mapping in the Ekofisk Field using a new form of collocated cokriging. In: Society of Petroleum Engineers Annual Technical Conference and Exhibition, Denver, pp. 21–30. <http://dx.doi.org/10.1190/1.1868153>.
- Dubrule, O., 2003. *Geostatistics for Seismic Data Integration in Earth Models*. Society of Exploration Geophysicists, URL <https://library.seg.org/doi/book/10.1190/1.9781560801962>.
- Emery, X., Parra, J., 2013. Integration of crosswell seismic data for simulating porosity in a heterogeneous carbonate aquifer. *J. Appl. Geophys.* 98, 254–264. <http://dx.doi.org/10.1016/j.jappgeo.2013.09.004>, URL <http://www.sciencedirect.com/science/article/pii/S0926985113002036>.
- Erdely, A., Díaz-Viera, M.A., 2010. Nonparametric and semiparametric bivariate modeling of petrophysical porosity-permeability dependence from well log data. In: Jaworski, P., Durante, F., Härdle, W., Rychlik, T. (Eds.), *Copula Theory and Its Applications*. In: Lecture Notes in Statistics, vol. 198, Springer, Berlin, Heidelberg, pp. 267–278. http://dx.doi.org/10.1007/978-3-642-12465-5_13.
- Erdely, A., Díaz-Viera, M.A., 2015. A vine and gluing copula model for permeability stochastic simulation. In: *Stochastic and Data Analysis Methods and Applications in Statistics and Demography*. pp. 273–281, URL https://www.academia.edu/23463707/A_vine_and_gluing_copula_model_for_permeability_stochastic_simulation.
- Figueiredo, L.P.D., Grana, D., Roisenberg, M., Rodrigues, B.B., 2019. Gaussian mixture Markov chain Monte Carlo method for linear seismic inversion. *Geophysics* 84 (3), <http://dx.doi.org/10.1190/geo2018-0529.1>.
- Gogoi, T., Chatterjee, R., 2019. Estimation of petrophysical parameters using seismic inversion and neural network modeling in Upper Assam basin, India. *Geosci. Front.* 10 (3), 1113–1124. <http://dx.doi.org/10.1016/j.gsf.2018.07.002>, URL <https://www.sciencedirect.com/science/article/pii/S1674987118301555>.
- Gómez-Hernández, J., Journel, A., 1993. Joint sequential simulation of multigaussian fields. In: Soares, A. (Ed.), *Geostatistics Tróia '92*. In: Quantitative Geology and Geostatistics, vol. 3, Springer, Dordrecht, http://dx.doi.org/10.1007/978-94-011-1739-5_8.
- Gräler, B., 2014. Modelling skewed spatial random fields through the spatial vine copula. *Spatial Stat.* 10, 87–102. <http://dx.doi.org/10.1016/j.spasta.2014.01.001>, URL <http://www.sciencedirect.com/science/article/pii/S2211675314000025>.
- Gräler, B., Pebesma, E., 2011. The pair-copula construction for spatial data: a new approach to model spatial dependency. *Procedia Environ. Sci.* 7, 206–211. <http://dx.doi.org/10.1016/j.proenv.2011.07.036>, URL <http://www.sciencedirect.com/science/article/pii/S1878029611001630>.
- Grana, D., 2018. Joint facies and reservoir properties inversion. *Geophysics* 83 (3), M15–M24. <http://dx.doi.org/10.1190/geo2017-0670.1>, URL <https://library.seg.org/doi/abs/10.1190/geo2017-0670.1>.
- Grana, D., Fjeldstad, T., Omre, H., 2017. Bayesian Gaussian mixture linear inversion for geophysical inverse problems. *Math. Geosci.* 49, <http://dx.doi.org/10.1007/s11004-016-9671-9>.
- Grana, D., Mukerji, T., Dvorkin, J., Mavko, G., 2012. Stochastic inversion of facies from seismic data based on sequential simulations and probability perturbation method. 77 (4) M53–M72. URL <https://doi.org/10.1190/geo2011-0417.1>.
- Grana, D., Rossa, E.D., 2010. Probabilistic petrophysical-properties estimation integrating statistical rock physics with seismic inversion. *Geophysics* 75, O21–O37. <http://dx.doi.org/10.1190/1.3386676>.
- Haslauer, C.P., Li, J., Bárdossy, A., 2010. Application of copulas in geostatistics. In: Atkinson, P.M., Lloyd, C.D. (Eds.), *GeoENV VII – Geostatistics for Environmental Applications*. Springer Netherlands, Dordrecht, pp. 395–404. http://dx.doi.org/10.1007/978-90-481-2322-3_34.
- Hernández-Maldonado, V., Díaz-Viera, M.A., Erdely, A., 2012. A joint stochastic simulation method using the bernstein copula as a flexible tool for modeling nonlinear dependence structures between petrophysical properties. *J. Pet. Sci. Eng.* 90–91, 112–123. <http://dx.doi.org/10.1016/j.petrol.2012.04.018>.
- Hernández-Maldonado, V., Díaz-Viera, M.A., Erdely, A., 2014. A multivariate bernstein copula model for permeability stochastic simulation. *Geofís. Int.* 53, 163–181. [http://dx.doi.org/10.1016/S0016-7169\(14\)71498-9](http://dx.doi.org/10.1016/S0016-7169(14)71498-9).
- Horta, A., Soares, A., 2010. Direct sequential co-simulation with joint probability distributions. *Math. Geosci.* 42 (3), 269–292. <http://dx.doi.org/10.1007/s11004-010-9265-x>.

- Iturrarán-Viveros, U., 2012. Smooth regression to estimate effective porosity using seismic attributes. *J. Appl. Geophys.* 76, 1–12. <http://dx.doi.org/10.1016/j.jappgeo.2011.10.012>, URL <http://www.sciencedirect.com/science/article/pii/S0926985111002485>.
- Iturrarán-Viveros, U., Parra, J.O., 2014. Artificial neural networks applied to estimate permeability, porosity and intrinsic attenuation using seismic attributes and well-log data. *J. Appl. Geophys.* 107, 45–54. <http://dx.doi.org/10.1016/j.jappgeo.2014.05.010>, URL <http://www.sciencedirect.com/science/article/pii/S092698511400144X>.
- Joe, H., 2014. Dependence Modeling with Copulas. In: Chapman & Hall/CRC Monographs on Statistics and Applied Probability, Chapman and Hall/CRC, URL <https://www.crcpress.com/Dependence-Modeling-with-Copulas/Joe/p/book/9781466583221>.
- Kazianka, H., Pilz, J., 2010. Spatial interpolation using copula-based geostatistical models. In: Atkinson, P.M., Lloyd, C.D. (Eds.), *GeoENV VII – Geostatistics for Environmental Applications*. Springer Netherlands, Dordrecht, pp. 307–319. http://dx.doi.org/10.1007/978-90-481-2322-3_27.
- Krupskii, P., Genton, M.G., 2019. A copula model for non-Gaussian multivariate spatial data. *J. Multivariate Anal.* 169, 264–277. <http://dx.doi.org/10.1016/j.jmva.2018.09.007>, URL <http://www.sciencedirect.com/science/article/pii/S0047259X18301696>.
- Lang, X., Grana, D., 2017. Geostatistical inversion of prestack seismic data for the joint estimation of facies and impedances using stochastic sampling from Gaussian mixture posterior distributions. *Geophysics* 82 (4), M55–M65. <http://dx.doi.org/10.1190/geo2016-0670.1>.
- Maurya, S., Singh, K., 2019. Predicting porosity by multivariate regression and probabilistic neural network using model-based and coloured inversion as external attributes: a quantitative comparison. *J. Geol. Soc. India* 93, 207–212. <http://dx.doi.org/10.1007/s12594-019-1153-5>, URL <https://link.springer.com/article/10.1007/s12594-019-1153-5>.
- Mendoza-Torres, F., Díaz-Viera, M., Erdely, A., 2017. Bernstein copula modeling for 2D discrete fracture network simulations. *J. Pet. Sci. Eng.* 156, 710–720. <http://dx.doi.org/10.1016/j.petrol.2017.06.021>, URL <http://www.sciencedirect.com/science/article/pii/S0920410517305193>.
- Moon, S., Lee, G.H., Kim, H., Choi, Y., Kim, H.-J., 2016. Collocated cokriging and neural-network multi-attribute transform in the prediction of effective porosity: A comparative case study for the second wall creek sand of the teapot dome field, Wyoming, USA. *J. Appl. Geophys.* 131, 69–83. <http://dx.doi.org/10.1016/j.jappgeo.2016.05.008>, URL <http://www.sciencedirect.com/science/article/pii/S0926985116301379>.
- Nagler, T., Czado, C., 2016. Evading the curse of dimensionality in nonparametric density estimation with simplified vine copulas. *J. Multivariate Anal.* 151, 69–89. <http://dx.doi.org/10.1016/j.jmva.2016.07.003>, URL <http://www.sciencedirect.com/science/article/pii/S0047259X16300471>.
- Nelsen, R.B., 2006. *An Introduction to Copulas*. In: Springer Series in Statistics, Springer-Verlag New York, <http://dx.doi.org/10.1007/0-387-28678-0>, URL <https://www.springer.com/us/book/9780387286594>.
- Parra, J., Emery, X., 2013. Geostatistics applied to cross-well reflection seismic for imaging carbonate aquifers. *J. Appl. Geophys.* 92, 68–75. <http://dx.doi.org/10.1016/j.jappgeo.2013.02.010>.
- Perez, J.M., Palacín, A.F., 1987. Estimating the quantile function by Bernstein polynomials. *Comput. Statist. Data Anal.* 5 (4), 391–397. [http://dx.doi.org/10.1016/0167-9473\(87\)90061-2](http://dx.doi.org/10.1016/0167-9473(87)90061-2), URL <http://www.sciencedirect.com/science/article/pii/0167947387900612>.
- Remy, N., Boucher, A., Wu, J., 2009. *Applied Geostatistics with SGeMS: A User's Guide*. Cambridge University Press, New York, <http://dx.doi.org/10.1017/CBO9781139150019>.
- Sancetta, A., 2007. Nonparametric estimation of distributions with given marginals via Bernstein-kantorovic polynomials: L 1 and pointwise convergence theory. *J. Multivariate Anal.* 98, 1376–1390.
- Sancetta, A., Satchell, S., 2004. The Bernstein copula and its applications to modeling and approximations of multivariate distributions. *Econometric Theory* 20 (03), 535–562, URL <https://EconPapers.repec.org/RePEc:cup:etheor:v:20:y:2004:i:03:p:535-562.20>.
- Shen, X., Zhu, Y., Song, L., 2008. Linear B-spline copulas with applications to non-parametric estimation of copulas. *Comput. Statist. Data Anal.* 52 (7), 3806–3819. <http://dx.doi.org/10.1016/j.csda.2008.01.002>, URL <http://www.sciencedirect.com/science/article/pii/S0167947308000066>.
- Sklar, A., 1959. Fonctions de répartition à n dimensions et leurs marges. *Publ. Inst. Stat. Univ. Paris* 8, 229–231.
- Soares, A., 2001. Direct sequential simulation and cosimulation. *Math. Geol.* 33 (8), 911–926. <http://dx.doi.org/10.1023/A:1012246006212>.
- Soares, A., 2005. Classification of mining reserves using direct sequential simulation. In: Leuangthong, O., Deutsch, C.V. (Eds.), *Geostatistics Banff 2004*. Springer Netherlands, Dordrecht, pp. 511–522. http://dx.doi.org/10.1007/978-1-4020-3610-1_51.
- Soares, A., Nunes, R., Azevedo, L., 2017. Integration of uncertain data in geostatistical modelling. *Math. Geosci.* 49 (2), 253–273. <http://dx.doi.org/10.1007/s11004-016-9667-5>.
- Stien, M., Kolbjørnsen, O., 2008. D-vine Creation of Non-Gaussian Random Fields. Norwegian Computing Center, URL <https://pdfs.semanticscholar.org/844b/5e07f320c62b5a42a0fdd970b9baf5a91d86.pdf>.
- Vejbæk, O.V., Kristensen, L., 2000. Downflank hydrocarbon potential identified using seismic inversion and geostatistics: Upper maastrichtian reservoir unit, dan field, danish central graben. *Pet. Geosci.* <http://dx.doi.org/10.1144/petgeo.6.1.1>.
- Verly, G.W., 1993. Sequential Gaussian cosimulation: A simulation method integrating general types of information. In: Soares, A. (Ed.), *Geostatistics Troia 92*. In: *Quantitative Geology and Geostatistics*, vol. 5, Springer, Dordrecht, pp. 543–554, URL https://link.springer.com/chapter/10.1007/978-94-011-1739-5_42.
- Xu, H., Sun, J., Russell, B., Innanen, K., 2016. Porosity prediction using cokriging with multiple secondary datasets. In: *Geoconvention. Optimizing Resources*. URL https://www.geoconvention.com/archives/2016/154_GC2016_Porosity_Prediction_using_Cokriging.pdf.
- Yarus, J.M., Chambers, R.L., 1994. *Stochastic Modeling and Geostatistics: Principles, Methods, and Case Studies*. American Association of Petroleum Geologists, <http://dx.doi.org/10.1306/CA3590>.
- Yenwongfai, H.D., Mondol, N.H., Faleide, J.I., Lecomte, I., Leutscher, J., 2017. Prestack inversion and multiattribute analysis for porosity, shale volume, and sand probability in the Havert Formation of the Goliat field, southwest Barents Sea. 5 (3). <http://dx.doi.org/10.1190/INT-2016-0169.1>. URL: <https://library.seg.org/doi/10.1190/INT-2016-0169.1>.